

FORMATION OF DIFFERENT ISOTOPOMERS OF CHLORONIUM IN THE INTERSTELLAR MEDIUM

LITON MAJUMDAR¹, ANKAN DAS¹, SANDIP K. CHAKRABARTI^{2,1}

¹Indian Centre for Space Physics, Chalanika 43, Garia Station Rd., Kolkata, 700084, India and

²S. N. Bose National Centre for Basic Sciences, Salt Lake, Kolkata, 700098, India

Draft version January 13, 2014

ABSTRACT

Main focus of this paper is to explore the possibility of findings two deuterated isotopomers of H_2Cl^+ (Chloronium) in and around the Interstellar Medium (ISM). Presence of Chloronium ion has recently been confirmed by Herschel Space Observatory's Heterodyne Instrument for the Far-Infrared (Neufeld et al. 2012). It observed para-chloronium towards six sources in the Galaxy. Existence of its deuterated isotopomers (HDCl^+ & D_2Cl^+) are till date not discussed in the literature. We find that these deuterated gas phase ions could be destroyed by various ion-molecular reactions, dissociative recombination (DR) and by cosmic rays (CR). We compute all the Ion-molecular (polar) reaction rates by using the parameterized trajectory theory and the Ion-molecular (non-polar) reaction rates by using the Langevin theory. For DR and CR induced reactions, we adopt two well behaved rate formulas. We also include these rate coefficients into our large gas-grain chemical network to study the chemical evolution of these species around the outer edge of the cold dense cloud. In order to study spectral properties of chloronium ion and its two deuterated isotopomers, we have carried out quantum chemical simulations. We calculated ground state properties of these species by employing second order Moller-Plesset perturbation theory (MP2) along with quadruple-zeta correlation consistent (aug-cc-pVQZ) basis set. Infrared and electronic absorption spectra of these species are calculated by using the same level of theory. MP2/aug-cc-pVQZ level of theory is used to report the different spectroscopic constants of these gas phase species. These spectroscopic constants are essential to predict rotational transitions of these species. Our predicted column densities of D_2Cl^+ , HDCl^+ along with the spectral information may enable their future identification around outer edges of cold dark clouds.

Subject headings: Astrochemistry, spectra, ISM: molecules, ISM: abundances, ISM: evolution, methods: numerical

1. INTRODUCTION

Cologne Database for Molecular Spectroscopy (CDMS) catalog (Muller et al. 2001; Müller et al. 2005) keeps records on discovered molecules in interstellar medium (ISM). According this catalog, more than 170 molecules have been detected so far in the ISM. Among them, there are some simple halides like, such as, HF, CF, AlF, HCl, HCl^+ , NaCl, KCl, AlCl, MgCl etc. Several works have been done in the past to model the chemistry of the chlorine-bearing molecules in both the diffuse and dense molecular clouds (Jura 1974; Dalgarno et al. 1974; van Dishoeck & Black 1986; Schilke et al. 1995; Federman et al. 1995; Amin 1996; Neufeld & Wolfire 2009). Various halogen elements such as fluorine and chlorine having solar abundances (3.6×10^{-8} and 3.2×10^{-7} respectively relative to total hydrogen nuclei (Asplund et al. 2009)) play an important role towards the formation of various hydrides in the ISM. Dissociation energy of most of the hydrides are less than that of the hydrogen molecule, only exceptions are the diatomic hydrides, such as, HF and diatomic hydride cations, such as, HCl^+ (Lis et al. 2010). Around an ISM, most of the halogen elements are biased to form hydrides (Neufeld et al. 2010). Huge abundances of HF and H_2Cl^+ are observed around the diffuse molecular clouds (Neufeld et al. 2010; Sonnentrucker et al. 2010; Lis et al. 2010).

The ionization potential of chlorine is slightly less than

that of the hydrogen and singly-ionized chlorine (Cl^+) can react exothermically with H_2 to form HCl^+ . This HCl^+ further interacts with H_2 to form H_2Cl^+ . These features are already known by theory of thermo chemistry of these species. Since Chloronium ion does not react with hydrogen molecule, dissociative recombination appears to be its main destruction route. Chloronium ion could also be destroyed by reacting with CO molecule. Main product of these destruction routes is hydrogen chloride (HCl). Theoretical modeling by considering the chlorine bearing molecules predicts that abundances of the Chloronium ions are significantly higher and could be observed. But surprisingly, before the launching of Herschel, among the Cl bearing molecules, only H^{35}Cl and H^{37}Cl were detected (Blake et al. 1985; Zmuidzinas et al. 1995; Schilke et al. 1995; Salez et al. 1996). Chemical modeling suggests that Chloronium ions could be very abundant around the diffuse interstellar medium. The detection of H_2Cl^+ was first reported towards NGC 6334I and Sgr B2(S) using the HIFI instrument (de Graauw et al. 2010) aboard the Herschel Space Observatory (Pilbratt et al. 2010). A follow up study by Neufeld et al. (2012) also detected H_2Cl^+ absorption towards Sgr A, W31C and detected Chloronium emission from two sources in the Orion Molecular Cloud 1 (the Orion Bar photodissociation region and Orion South condensation) and the young massive star AFGL 2591.

Despite these overwhelmingly significant observational evidences, till date, no deuterated forms of H_2Cl^+ have been observed in the ISM. This motivates

¹ankan.das@gmail.com

us to model the formation/destruction of different forms of deuterated H_2Cl^+ in the ISM. Importance of interstellar grains in producing simpler molecules has been widely described by several authors such as Stantcheva et al. (2002); Hasegawa, Herbst & Leung (1992); Chakrabarti et al. (2006a,b); Das et al. (2008a,b); Das, Acharyya & Chakrabarti (2010); Das et al. (2011). These studies indicate that dusts could play a crucial role for deciding chemical compositions around any molecular cloud. In order to understand complete picture of how molecules are formed in or around an ISM, we used our large gas-grain chemical model (Das et al. 2013a; Majumdar et al. 2012, 2013a,b).

Majumdar et al. (2013a,b) & Das et al. (2013b) performed quantum chemical simulations to find out various chemical properties of some interstellar species. In the current paper, we carry out a similar types of quantum chemical calculations to find out the spectral information (infrared, electronic and rotational) of different deuterated isotopomers of Chloronium ion. We have also provided detailed information about rotational transitions of these species (in the format of JPL catalog). Such a study would be extremely helpful for the identification of these species around ISMs.

The plan of this paper is the following: In Section 2, the models and the computational details are presented. Implications of the results are discussed in Section 3. Finally, in Section 4, we draw our conclusions. In Appendix A, we tabulate relevant parameters for rotational spectroscopy of one of the isotopomer of H_2Cl^+ in the format of JPL catalog.

2. COMPUTATIONAL DETAILS

2.1. Quantum chemical simulations and derived spectral parameters

We study spectral properties of interstellar chloronium by first optimizing the geometry of chloronium using second order Moller-Plesset perturbation theory (MP2) along with aug-cc-pVQZ basis set. MP2 theory is a special case of more general many-body perturbation theory (Puzzarini, Stanton & Gauss 2010). For calculations where only valence electrons are correlated (i.e., frozen core calculation), standard cc-pVXZ sets with $X = \text{D, T, Q, 5}$ and 6 are recommended (Puzzarini, Stanton & Gauss 2010). Because of this, we use here aug-cc-pVQZ basis set along with MP2 method. Vibrational frequencies of H_2Cl^+ and its two deuterated isotopomers; D_2Cl^+ and HDCl^+ are computed by determining second derivative of energy with respect to Cartesian nuclear coordinates and then transforming into mass-weighted coordinates. This transformation is valid only at a stationary point.

Vibrational frequencies of these species in the ice phase are also obtained by using the same level of theory. Vibrational spectra of any chemical species are significantly affected by the type of solvent used in the simulation. In our modeling purpose, here we have used Polarizable Continuum Model (PCM) with integral equation formalism variant (IEFPCM) as a default Self-consistent Reaction Field (SCRF) method (Tomasi et al., 2002; Tomasi, Mennucci & Cami 2005; Tomasi, Mennucci & Cancès 1999; Pascual-Ahuir et al.

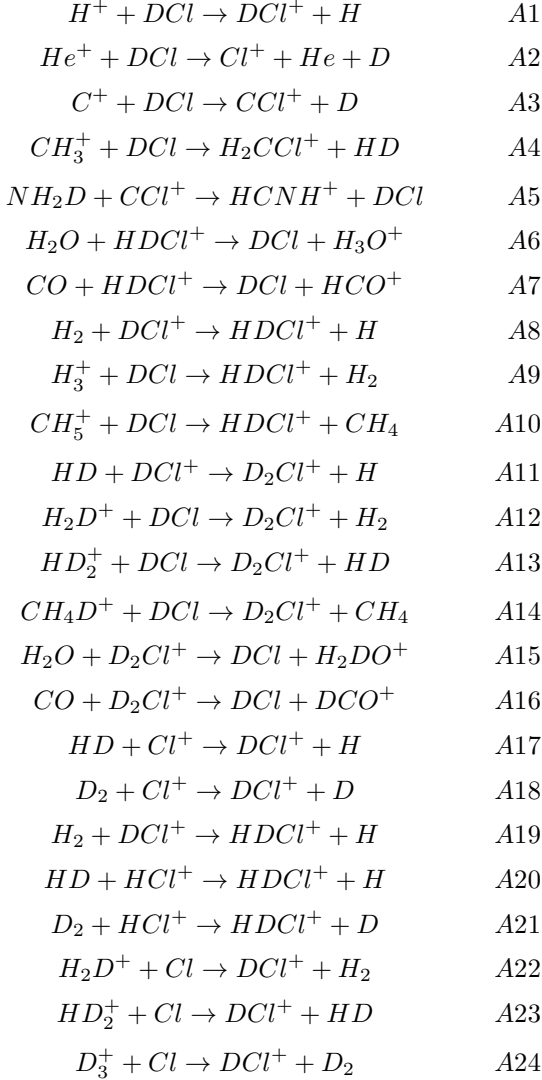
1994). SCRF method in Gaussian 09W program is used to perform calculations in presence of a solvent by placing the solute in a cavity within a solvent reaction field. Following Das et al. (2013b), here too we have considered simple as well as mixed ice. By simple ice, we mean ice made from water molecule only and by mixed ice, we mean the ice made from water, methanol and carbon dioxide. Observations around cold dense region of molecular cloud reveal that $\sim 90\%$ of interstellar grain mantle could be covered by H_2O , CH_3OH and CO_2 (Keane et al. 2001). We have also carried out quantum chemical simulation (time dependent density functional theory) to find out electronic absorption spectrum of these species in the gas phase as well as simple ice and mixed ice phase using the IEFPCM model.

An important key for the successful identification of different forms of chloronium in the interstellar space depends on the availability of accurate predictions of spectroscopic constants (rotational and distortional constants). Our computed rotational spectral information for interstellar chloronium is based on equilibrium geometry obtained at MP2/aug-cc-pVQZ level, i.e., with the consideration of core correlation and vibrational corrections to the rotational constants. Centrifugal distortion constants are computed from harmonic and anharmonic force fields obtained at MP2/aug-cc-pVQZ levels of theory. In addition, computed components of dipole moment were used to predict relative intensities of rotational transitions. These spectroscopic constants are essential to predict spectrum of different forms of H_2Cl^+ and this can be done by following techniques described in Das et al. (2013b). It used Pickett's 'SPCAT' program (Pickett et al. 1991) for this purpose. Two main files, namely, 'file.var' and 'file.int' are required for the SPCAT program. Specified format of these two files were explained in detail in Pickett et al. (1991). Information regarding rotational constants, quadrupole coupling constants and distortional constants are given in 'var' file. Contents of 'var' file could directly be generated from Gaussian 09 program. 'int' file is the intensity file and it is prepared according to the prescribed format of 'SPCAT program'. This file contains maximum and minimum number of rotational states, partition function, rotational temperature and dipole moment of the molecule.

2.2. Chemical Modeling

In order to study various forms of chloronium in an interstellar medium (ISM), we have developed a chemical model which includes gas phase as well as grain surface chemical network. Our gas phase chemical network consists of a network of Woodall et al. (2007) and deuterated network used in Das et al. (2013b). In addition, we include some deuterated reactions by following Roberts & Millar (2000); Albertsson et al. (2013). We include certain new reactions for formation and destruction of various forms of chloronium and its related species. Our present gas phase chemical network consists of 6180 reactions and present surface chemical network consists of 285 reactions. Except molecular hydrogen and Helium, depletion of all gas phase neutral species onto the grain surface are considered with a sticking probability of unity. The reason for ignoring this for H_2 and He is that according to Leitch & Williams (1985), the sticking coefficient of $\text{H}_2 \sim 0$ and Roberts & Millar (2000)

argued that Helium would not stick to the grain at all. Following is the list of reactions which are considered in our network for the formation/destruction of deuterated isotopomers of chloronium ion.



Reaction A1 is a charge exchange type reaction. Rate coefficient for this reaction is assumed to be similar to the rate coefficient adopted for $H^+ + HCl \rightarrow HCl^+ + H$ in Woodall et al. (2007). Reactions A2 - A24 are Ion-neutral type reactions. According to Herbst (2006), rate coefficients for ion-molecular reactions can be determined by using capture theories (in which translational energy of reactants must only surpass a long-range centrifugal barrier for a reaction to occur). The collision rate coefficient between an ion and non-polar neutral molecule can be determined by using so-called Langevin collision rate;

$$k = 2\pi e \sqrt{\alpha_d / \mu}, \quad (1)$$

where, e is electronic charge, α_d is polarizability of neutral non-polar molecule, μ is reduced mass of reactants. But for polar neutral species, a complex situation arises due to attraction between a charge and a rotating permanent dipole moment. In these cases, extensive trajectory calculations have been carried out by Su & Chesnavich (1982) to predict rate coefficients

(k_{cap}) of ion-polar molecule capture collisions. According to Woon & Herbst (2009), Su-Chesnavich formula can be written in two different ways and both of which uses a parameter $x = \mu_D / \sqrt{(2\alpha kT)}$ where k is Boltzman constant & T is the temperature. The ion-dipole (k_{cap}) rates can be parameterized using following equations:

$$k_{cap} = (0.4767x + 0.6200)k_L, \quad (2)$$

and

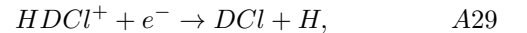
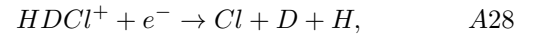
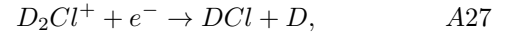
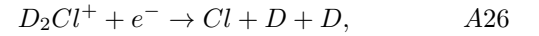
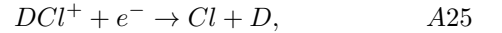
$$k_{cap} = [(x + 0.5090)^2 / 10.526 + 0.9754]k_L. \quad (3)$$

Equation 2 is used if $x \geq 2$ and Eqn. 3 is used if $x < 2$. Note that for $x = 0$, it reduces to the Langevin expression. Alternatively, the expression can be written in powers of temperature T . For example, when $x \geq 2$,

$$k_{cap} = c_1 + c_2 T^{-1/2}, \quad (4)$$

where, $c_1 = 0.62k_L$ and $c_2 = (0.4767\mu_D / \sqrt{(2\alpha K)})k_L$. If the second term in Eqn. 4 is much greater than the first term, the expression has $T^{-1/2}$ dependence which is used in both the UMIST and OSU databases. We took values of polarizability and dipole moments of neutral species by following Woon & Herbst (2009). They optimized equilibrium structures at RCCSD(T)/aug-cc-pVTZ level of theory using finite field approach to obtain dipole moment and dipole polarizability components. According to their calculations, values of the polarizabilities (α) for HCl, H₂O, H₂, CO, NH₃ are to be 2.538, 1.406, 0.773, 1.951 and 2.087 Å³ respectively and values of the Dipole moments (μ_D) for HCl, H₂O, H₂, CO, NH₃ are to be 1.075, 1.845, 0, 0.101, 1.519 Debye respectively. Now, computation of polarizability and dipole moments depend on the derivatives of electronic energy with respect to external electric field. This electronic energy is not dependent on the mass of the nuclei as calculations are based on Born-Oppenheimer approximation. But experimental difference arises mostly from difference in vibrationally averaged structure. In our case, polarizability and dipole moments of HD, D₂, DCl, NH₂D are assumed to be similar to their hydrogenated counter part. Plugging these values (polarizability and dipole moment of the neutral species and reduced mass of the reactants) in above equations, we calculated reaction rates for the ion-neutral reactions (A2-A24).

Molecular ions could be destroyed by the following dissociative recombination reactions:



In the absence of experimentally determined rate coefficients, following Neufeld & Wolfire (2009), we use Eqns. 5 & 6 for computation of DR rate coefficients (A25-A29) for diatomic and triatomic molecular ions, namely,

$$k = 2 \times 10^{-7} (T/300)^{-1/2} \text{ cm}^3 \text{ s}^{-1}, \quad (5)$$

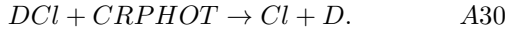
and

$$k = 1.2 \times 10^{-7} (T/300)^{-0.85} \text{ cm}^3 \text{ s}^{-1}. \quad (6)$$

TABLE 1
INITIAL ABUNDANCES USED RELATIVE TO TOTAL HYDROGEN NUCLEI.

Species	Abundance
H ₂	5.00×10^{-01}
He	1.00×10^{-01}
N	2.14×10^{-05}
O	1.76×10^{-04}
H ₃ ⁺	1.00×10^{-11}
C ⁺	7.30×10^{-05}
S ⁺	8.00×10^{-08}
Si ⁺	8.00×10^{-09}
Fe ⁺	3.00×10^{-09}
Na ⁺	2.00×10^{-09}
Mg ⁺	7.00×10^{-09}
P ⁺	3.00×10^{-09}
Cl ⁺	4.00×10^{-09}
e ⁻	7.31×10^{-05}
HD	1.6×10^{-05}

Following the destruction pathways of HCl (Woodall et al. 2007), we have assumed that DCl could also be destroyed by Cosmic ray induced (CRPHOT) Photo reactions;

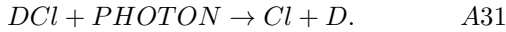


The rate of Cosmic ray induced photo-reaction (A30) could be adopted as follows:

$$k_{CR}(T) = \alpha(T/300)^\beta \gamma / (1 - \omega) \text{ s}^{-1}, \quad (7)$$

where, cosmic-ray ionization rate is denoted by α , photo reaction probability per cosmic ray ionization is denoted by γ and ω denotes reflection coefficients of dust grain in far UV. Following reaction $HCl + CRPHOT \rightarrow H + Cl$ in Woodall et al. (2007), here too we assume that $\alpha = 1.3 \times 10^{-17}$, $\beta = 0$, $\gamma = 305$ and $\omega = 0.6$.

DCl could also be dissociated by following interstellar photo reaction (PHOTON);



The rate coefficient for the reaction A31 could be calculated by using following relation:

$$k_{Phot} = \alpha \exp(-\gamma A_V) \text{ s}^{-1}, \quad (8)$$

where, A_V is the visual extinction and $\gamma = 1.8$ is used following the reaction $HCl + PHOTON \rightarrow Cl + H$ in Woodall et al. (2007).

In our model, we assume that gas and grains are coupled through accretion and thermal/cosmic ray evaporation processes. To model the environment of the outer edge of a dense interstellar cloud or a diffuse cloud, we use $T=10\text{K}$, $n_H = 10^3 - 10^4 \text{ cm}^{-3}$, $A_V = 0.01 - 10$ magnitude. Following Roberts & Millar (2000), in Table 1, initial elemental abundances relative to the total hydrogen nuclei is shown. This type of initial abundances are often adopted for the cold & dark cloud. All computed/estimated rate coefficients (A1-A31) are provided in Table 2 for $T=10\text{K}$, $A_V = 10$.

3. RESULTS AND DISCUSSIONS

3.1. Chemical properties

Interstellar chloronium (H_2Cl^+) is an asymmetric top with C_{2v} symmetry. We performed quantum chemical simulation (MP2/aug-cc-pVQZ level of theory) for geometry optimization and energy calculation of chloronium ion. Ground state energies of H_2Cl^+ in gas and

ice phases are found to be -460.55382 a.u. , -460.67002 a.u. (1 atomic unit = 27.21 eV) respectively. Due to solute-solvent electrostatic interaction (dipole level), ground state energy in ice phase is found to be lower than ground state energy in gas phase. The solvent effect also brings changes in geometrical parameters of these species. Our results confirm that polarization of solute by continuum has important effects on absolute and relative solvation energies, which in turn changes the energy of respective species. The ground state energy of D_2Cl^+ and HDCl^+ are found to be similar to the ground state energy of H_2Cl^+ in gas and in ice phases. This is due to the fact that ground state energy and structure calculations are made by using Born-Oppenheimer approximation so isotopic mass is not a factor in the Hamiltonian. The dipole moment of chloronium in gas and in ice phases are found to be 1.98 Debye and 2.2024 Debye respectively. The dipole moment of chloronium has been estimated as 1.89 Debye in *ab initio* calculations performed by Müller (2008). According to Puzzarini, Stanton & Gauss (2010), additional splitting in rotational spectrum is governed by nuclear quadrupole coupling of molecules. Moreover, according to them, quantum chemical calculations could be extremely helpful for fine structure analysis because it could provide electric-field gradient at corresponding nuclei. In Table 3, we show a comparison of experiment and theoretical ground state quadrupole coupling constants of chlorine H_2Cl^+ for Mp2/aug-cc-pVQZ level of theory. Also, for the first time, we provide quadrupole coupling constants of chlorine in D_2Cl^+ , HDCl^+ in the same table.

3.2. Chemical evolution and deuterium enrichment

In Fig. 1, chemical evolution of chloronium ion and related species are shown. To mimic the interstellar scenario, we consider $n_H = 10^4 \text{ cm}^{-3}$, $A_V = 10$ and $T=10\text{K}$. It is assumed that initially all deuteriums are locked in the form of HD. Initial abundances of HD and H_2 are taken to be 1.6×10^{-5} and 0.5 respectively (Table 1) with respect to total number of hydrogen nuclei. This implies an initial fractionation ratio of 3.2×10^{-5} . Unless otherwise stated, we use this initial fractionation ratio in all our simulations. In our gas-grain model, we assume that all the neutral species could be depleted to icy grain with a sticking coefficient of unity. Depleted species are allowed to populate the gas phase via thermal evaporation

TABLE 2
FORMATION/DESTRUCTION OF DEUTERATED CHLORONIUM IONS AND RELATED SPECIES

Reaction	Reaction Type	Rate coefficients
$H^+ + DCl \rightarrow DCl^+ + H$ (A1)	Charge Exchange	$1.1 \times 10^{-10} \text{ cm}^3 \text{ s}^{-1}$
$He^+ + DCl \rightarrow Cl^+ + He + D$ (A2)	Ion-neutral	$1.8 \times 10^{-8} \text{ cm}^3 \text{ s}^{-1}$
$C^+ + DCl \rightarrow CCl^+ + D$ (A3)	Ion-neutral	$8.3 \times 10^{-10} \text{ cm}^3 \text{ s}^{-1}$
$CH_3^+ + DCl \rightarrow H_2CCl^+ + HD$ (A4)	Ion-neutral	$7.7 \times 10^{-09} \text{ cm}^3 \text{ s}^{-1}$
$NH_2D^+ + CCl^+ \rightarrow HCNH^+ + DCl$ (A5)	Ion-neutral	$9.5 \times 10^{-09} \text{ cm}^3 \text{ s}^{-1}$
$H_2O + HDCl^+ \rightarrow DCl + H_3O^+$ (A6)	Ion-neutral	$1.2 \times 10^{-08} \text{ cm}^3 \text{ s}^{-1}$
$CO + HDCl^+ \rightarrow DCl^+ + HCO^+$ (A7)	Ion-neutral	$2.5 \times 10^{-10} \text{ cm}^3 \text{ s}^{-1}$
$H_2 + DCl^+ \rightarrow HDCl^+ + H$ (A8)	Ion-neutral	$1.5 \times 10^{-09} \text{ cm}^3 \text{ s}^{-1}$
$H_3^+ + DCl \rightarrow HDCl^+ + H_2$ (A9)	Ion-neutral	$1.5 \times 10^{-08} \text{ cm}^3 \text{ s}^{-1}$
$CH_5^+ + DCl \rightarrow HDCl^+ + CH_4$ (A10)	Ion-neutral	$7.3 \times 10^{-09} \text{ cm}^3 \text{ s}^{-1}$
$HD + DCl^+ \rightarrow D_2Cl^+ + H$ (A11)	Ion-neutral	$1.2 \times 10^{-09} \text{ cm}^3 \text{ s}^{-1}$
$H_2D^+ + DCl \rightarrow D_2Cl^+ + H_2$ (A12)	Ion-neutral	$1.3 \times 10^{-08} \text{ cm}^3 \text{ s}^{-1}$
$HD_2^+ + DCl \rightarrow D_2Cl^+ + HD$ (A13)	Ion-neutral	$1.2 \times 10^{-08} \text{ cm}^3 \text{ s}^{-1}$
$CH_4D^+ + DCl \rightarrow D_2Cl^+ + CH_4$ (A14)	Ion-neutral	$7.2 \times 10^{-09} \text{ cm}^3 \text{ s}^{-1}$
$H_2O + D_2Cl^+ \rightarrow DCl + H_2DO^+$ (A15)	Ion-neutral	$1.2 \times 10^{-08} \text{ cm}^3 \text{ s}^{-1}$
$CO + D_2Cl^+ \rightarrow DCl + DCO^+$ (A16)	Ion-neutral	$2.5 \times 10^{-10} \text{ cm}^3 \text{ s}^{-1}$
$HD + Cl^+ \rightarrow DCl^+ + H$ (A17)	Ion-neutral	$1.2 \times 10^{-09} \text{ cm}^3 \text{ s}^{-1}$
$D_2 + Cl^+ \rightarrow DCl^+ + D$ (A18)	Ion-neutral	$1.1 \times 10^{-09} \text{ cm}^3 \text{ s}^{-1}$
$H_2 + DCl^+ \rightarrow HDCl^+ + H$ (A19)	Ion-neutral	$1.5 \times 10^{-09} \text{ cm}^3 \text{ s}^{-1}$
$HD + HCl^+ \rightarrow HDCl^+ + H$ (A20)	Ion-neutral	$1.2 \times 10^{-09} \text{ cm}^3 \text{ s}^{-1}$
$D_2 + HCl^+ \rightarrow HDCl^+ + D$ (A21)	Ion-neutral	$1.1 \times 10^{-09} \text{ cm}^3 \text{ s}^{-1}$
$H_2D^+ + Cl \rightarrow DCl^+ + H_2$ (A22)	Ion-neutral	$1.0 \times 10^{-09} \text{ cm}^3 \text{ s}^{-1}$
$HD_2^+ + Cl \rightarrow DCl^+ + HD$ (A23)	Ion-neutral	$1.0 \times 10^{-09} \text{ cm}^3 \text{ s}^{-1}$
$D_3^+ + Cl \rightarrow DCl^+ + D_2$ (A24)	Ion-neutral	$1.0 \times 10^{-09} \text{ cm}^3 \text{ s}^{-1}$
$DCl^+ + e^- \rightarrow Cl + D$ (A25)	Dissociative Recombination	$6.0 \times 10^{-6} \text{ s}^{-1}$
$D_2Cl^+ + e^- \rightarrow Cl + D + D$ (A26)	Dissociative Recombination	$1.2 \times 10^{-5} \text{ s}^{-1}$
$D_2Cl^+ + e^- \rightarrow DCl + D$ (A27)	Dissociative Recombination	$1.2 \times 10^{-5} \text{ s}^{-1}$
$HDCl^+ + e^- \rightarrow Cl + D + H$ (A28)	Dissociative Recombination	$1.2 \times 10^{-5} \text{ s}^{-1}$
$HDCl^+ + e^- \rightarrow DCl + H$ (A29)	Dissociative Recombination	$1.2 \times 10^{-5} \text{ s}^{-1}$
$DCl + CRPHOT \rightarrow Cl + D$ (A30)	Cosmic ray induced Photodissociation	$9.9 \times 10^{-15} \text{ s}^{-1}$
$DCl + PHOTON \rightarrow Cl + D$ (A31)	Photo-dissociation	$1.7 \times 10^{-17} \text{ s}^{-1}$

TABLE 3
THEORETICAL AND EXPERIMENTAL QUADRUPOLE COUPLING CONSTANTS OF CHLORINE IN H_2Cl^+ , D_2Cl^+ , $HDCl^+$.

Species	Constants	Theoretical values in MHz	Experimental values in MHz ^a
H_2Cl^+	χ_{aa}	-51.8851	-53.44
	χ_{bb}	-14.3463	-15.71
	χ_{cc}	66.2314	69.15
	χ_{ab}	-0.4689	-
$HDCl^+$	χ_{aa}	-39.2014	-
	χ_{bb}	-27.1076	-
	χ_{cc}	66.3090	-
	χ_{ab}	17.4213	-
D_2Cl^+	χ_{aa}	-51.8863	-
	χ_{bb}	-14.3470	-
	χ_{cc}	66.2333	-
	χ_{ab}	-0.3328	-

^a Saito & Yamamoto (1988)

and cosmic ray evaporation processes. Due to depletion of neutral species, rate of production of their relative ions are decreased. Dissociative recombination processes then lead to destruction of these ionic species. As a result, abundances of these ions are decreased. In our simulation, we evolved our chemical code till a time comparable to the life time of a generic molecular cloud ($\sim 10^7$ years). From Fig. 1, it is clear that most of the species attain peak values near $\sim 10^5$ years. In the literature, a number of theoretical models attempted to find time variation of physical properties of protostars since the beginning of gravitational collapse (Smith 1998; Myers et al. 1998). Time sequence of evolutionary stages determined by various models are more or less similar but their estimates of absolute ages vary significantly (Emprechtinger et al.

2008). According to Froebrich et al. (2005), the absolute age for Class 0/I borderline objects, for example, varies between 10^4 and a few times 10^5 years. Our simulation results in Fig. 1 shows that within this time frame, some species will attain peak values. It is also evident that one of the isotopomers of H_2Cl^+ (i.e., $HDCl^+$ from Fig. 1) is reasonably abundant within this time frame of collapse. So it is expected to be observed with ALMA, for example.

Following Shalabiea & Greenberg (1994) and Das et al. (2011), the column density of a species could be calculated using the following relation:

$$N(A) = n_H x_i R, \quad (9)$$

where, n_H is the total hydrogen number density, x_i is the

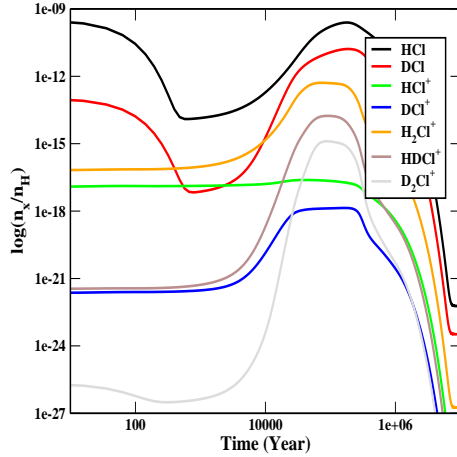


FIG. 1.— Time evolution of the Chloronium ion and its related species.

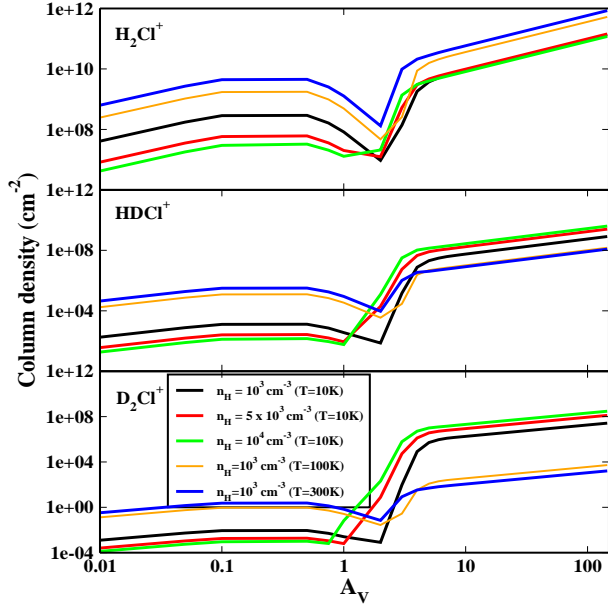


FIG. 2.— Variation of peak column densities with visual extinction parameter (A_V).

abundance of the i^{th} species and R is the path length along the line of sight ($= \frac{1.6 \times 10^{21} \times A_V}{n_H}$). According to Lis et al. (2010), H_2Cl^+ is predicted to be the most abundant in those environments where ultraviolet radiation is strong (i.e., in diffuse clouds, or near surfaces of dense clouds that are illuminated by nearby O and B stars). In Fig. 2, we mimic these features by varying visual extinction parameter (A_V) from 0.1 to 145. This high value of visual extinction ($A_V = 145$) could be used for W33A (Allamandola, Sandford & Tielens 1992). Variation of peak column densities of chloronium ion and its isotopomers are shown for different number density clouds (10^3 - 10^4 cm^{-3}). Abundance of H_2Cl^+ roughly remains constant beyond $A_V = 5$. From Eqn. 9 it is clear that the column density is directly proportional to A_V . As the abundance (x_i) remains constant be-

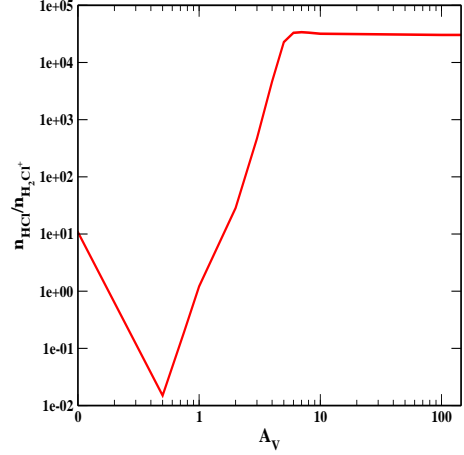


FIG. 3.— Variation of HCl/H_2Cl^+ column density ratio with A_V

yond $A_V = 5$, peak column densities increase linearly. For $A_V < 4$, peak column densities are heavily affected. Column densities are maximum around heavily shielded region ($A_V > 4$). Lis et al. (2010) computed column density of H_2Cl^+ to be $2.2 - 3.4 \times 10^{13} cm^{-2}$ along NGC 6334I by assuming 5K excitation temperature. Neufeld & Wolfire (2009) identified H_2Cl^+ around photo dissociation regions. According to their prediction, column density of H_2Cl^+ around a photo dissociation region ($n_H \sim 10^4 cm^{-3}$, $\kappa_{UV} \sim 10^4$) would be $\sim 2.6 \times 10^{11} cm^{-2}$. κ_{UV} is the UV radiation field which is normalized with respect to the mean interstellar value by Draine (1978). Neufeld & Wolfire (2009) also predicted column density of chloronium $\sim 3 \times 10^{11} cm^{-2}$ for the conditions which could be applicable to the environment of Orion Bar PDR ($n_H \sim 6 \times 10^4 cm^{-3}$ and $\kappa_{UV} \sim 3 \times 10^4$). Their predicted column density was also 100 times smaller than what is found in recent observation by Lis et al. (2010). Neufeld et al. (2012) mentioned that this theoretically predicted value should not be compared directly with the observed values because theoretical prediction was for the perpendicular column density whereas Orion Bar PDR was observed nearly edge-on. They expect that geometrical enhancement in the observed value of the column density by a factor of 4 could be possible. In our case, we find a peak column density of $H_2Cl^+ \sim 1.3 \times 10^{11} cm^{-2}$ in between $A_V = 0.1 - 145$, $n_H = 10^3 - 10^4 cm^{-3}$ and $T = 10K$. We also carried out our simulation at higher temperature to find out effects of temperature on the formation of chloronium ion. For this case, we assumed $n_H = 10^3 cm^{-3}$ and varied visual extinction (A_V) in between 0.1 – 145 for temperature 100K and 300K respectively (Fig. 2). From Fig. 2, it is evident that column density of chloronium ion increases with temperature and we have the maximum column density of $8.49 \times 10^{11} cm^{-2}$ at 300K. Column densities of deuterated forms of chloronium ion are also heavily affected by increase in temperature. For $A_V < 2$, column densities of these deuterated ions increases whereas for $A_V > 2$ they are found to decrease when compared to the $T=10K$ case.

Lis et al. (2010) derived HCl/H_2Cl^+ column density ratios to be in the range $\sim 1 - 10$, for diffuse and dense photon dominated regions (PDRs). In Fig. 3, we show variation of HCl/H_2Cl^+ column density ratio with A_V . For $A_V < 2$ (i.e., for the strong radiation field), our

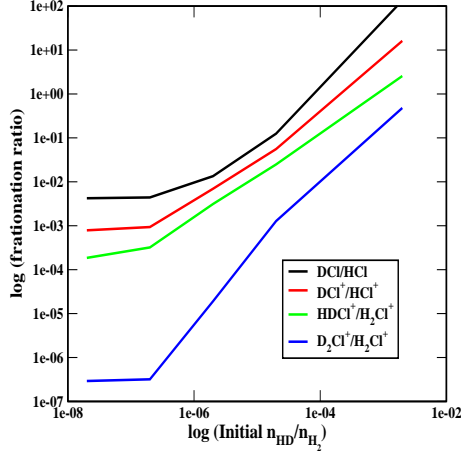


FIG. 4.— Variation of fractionation ratio with initial HD/H₂ ratio

results are in line with observation. For this case, we assumed $n_H = 10^4 \text{ cm}^{-3}$, $T = 10\text{K}$, and HCl/H₂Cl⁺ column density ratio was taken after the simulation time scale of $\sim 10^7$ year.

In Fig. 4, we show variation of fractionation ratio of HCl, HCl⁺ and H₂Cl⁺ with initial n_{HD}/H_2 ratio. For this case, we assumed $n_H = 10^4 \text{ cm}^{-3}$, $A_V = 10$ and $T = 10\text{K}$. HCl and HCl⁺ are found to be heavily fractionated, always crossing elemental D/H ratio ($\sim 10^{-5}$, Linsky et al., 1995). It is interesting to note that in our simulations, HDCl⁺/H₂Cl⁺ column density ratio is always above the elemental D/H ratio. Fractionation ratio of D₂Cl⁺ molecule crossing the elemental D/H ratio beyond initial n_{HD}/H_2 ratio 10^{-6} . As H₂Cl⁺ molecule is heavily fractionated, we strongly suggest to look for HDCl⁺ molecules in the same molecular clouds where H₂Cl⁺ molecule was already been observed.

3.3. Spectral Analysis

We now turn to spectral properties of H₂Cl⁺ and two of its isotopomers. For vibrational spectra, we compute infrared peak positions with their absorbance in gas phase as well as in water ice and mixed ice phases. In Table 4, we present these for H₂Cl⁺ and two of its isotopomers, namely, D₂Cl⁺ and HDCl⁺. We find that the most intense mode of H₂Cl⁺ in the gas phase appears nearly at 2779.83 cm^{-1} . This peak is shifted in the ice phase (water ice) by nearly 42 cm^{-1} and appears at 2822.06 cm^{-1} . The second strongest peak in the gas phase appears at 2789.60 cm^{-1} . It is also shifted in the ice phase. To have a more realistic condition, instead of only the water ice, we have considered a mixed ice mantle, which contains 70% water, 20% methanol and 10% CO₂ molecules (Keane et al. 2001; Das et al. 2011; Majumdar et al. 2013a,b; Das et al. 2013b). Gaussian 09W program uses a dielectric constant of water to be ~ 78.5 . For the case of mixed ice, we put the dielec-

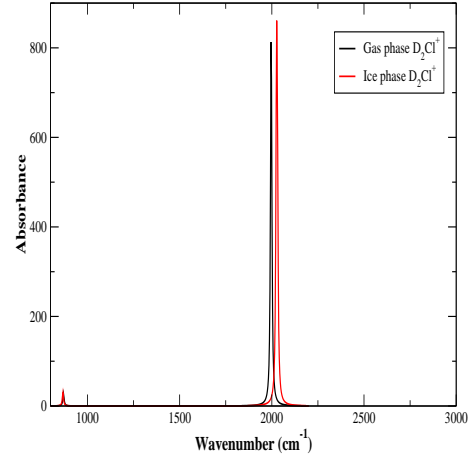


FIG. 5.— Infrared spectrum of D₂Cl⁺ in gas as well as in ice phase.

tric constant of the medium to be 61, which is calculated by taking an weighted average of the dielectric constants of H₂O, CH₃OH and CO₂. We note that the most intense peak in gas phase is shifted in mixed ice also (Table 4). Isotope effects on chemical shifts is caused by differences in vibrational modes due to different isotope masses. Each of the H₂Cl⁺, D₂Cl⁺ and HDCl⁺ molecules has a unique spectrum because substitution of isotope changes reduced mass of corresponding molecule. We find that the most intense mode of D₂Cl⁺ in gas phase appears at 1995.63 cm^{-1} . This peak is shifted in ice phase by 29.82 cm^{-1} , i.e., at 2025.45 cm^{-1} . The second strongest peak in gas phase which appears at 1998.19 cm^{-1} is also shifted in ice phase and appears at 2030.55 cm^{-1} . The most intense peak in gas phase is similarly shifted in mixed solvated grain. Infrared peak positions with their absorbance in gas phase as well as in ice and mixed ice phases are marked for D₂Cl⁺ and HDCl⁺ in Table 4. In Fig. 5 and in Fig. 6, we show how the isotopic substitution (D₂Cl⁺ and HDCl⁺) plays a part in vibrational progressions of H₂Cl⁺ in gas phase and in ice phase. Our results clearly show differences between spectroscopic parameters computed for interstellar chloronium ion in gas phase and in ice phase. These differences can be explained due to electrostatic effects that are often much less important for species placed in a solvent with high dielectric constant than they are in gas phase (Foresman & Frisch 1996).

In Table 5, we summarize our calculated theoretical values of rotational and quartic centrifugal distortion constants for H₂Cl⁺, D₂Cl⁺ and HDCl⁺ in gas phase. Calculated constants are corrected for each vibrational state as well as vibrationally averaged structures. MP2/aug-cc-pVQZ level of theory has been used to perform these calculations for gas phase H₂Cl⁺, D₂Cl⁺ and HDCl⁺. We compare our calculated spectroscopic constants (A, B, C, D_{JK}) of H₂Cl⁺ with Saito & Yamamoto (1988) in Table 5. In order to summarize the outcome of our calculations about rotational spectroscopy, we prepare our spectral information for one of the isotopologues of H₂Cl⁺ (HDCl⁺) as per guidelines of JPL (Table A1 of Appendix A). Computed transitions are falling in be-

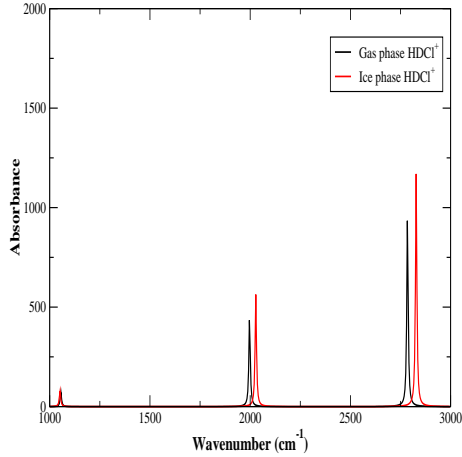


FIG. 6.— Infrared spectrum of HDCl^+ in gas as well as in ice phase.

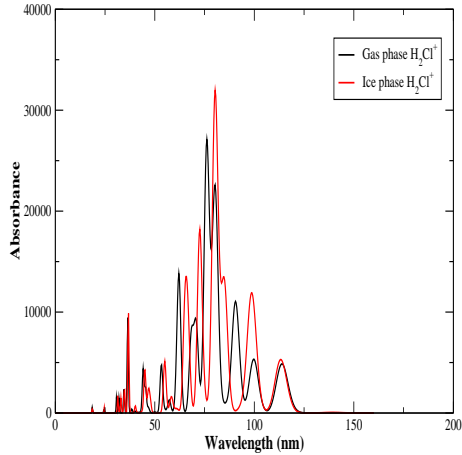


FIG. 7.— Electronic absorption spectrum of H_2Cl^+ in gas phase and in ice phase.

tween the 3 to 9 bands of ALMA (84 - 720 GHz). Our

computed column density also suggests that it could also be observed around the similar region, where H_2Cl^+ was observed.

Different electronic absorption spectral parameters of H_2Cl^+ in gas phase are given in Table 6. In gas phase, the spectrum is characterized by five intense peaks at wavelengths of 90.6, 80.3, 76.1, 62.3, 36.4 nm (Fig. 7). These intense peaks are assigned due to HOMO-LUMO transitions. These transitions correspond to $\text{H-0} \rightarrow \text{L+2}$, $\text{H-2} \rightarrow \text{L+0}$, $\text{H-1} \rightarrow \text{L+3}$, $\text{H-2} \rightarrow \text{L+2}$, $\text{H-0} \rightarrow \text{L+13}$. Depending on the composition of interstellar grain mantle, peak positions in ice phase are shifted. These features are presented in Table 6 with corresponding transition details. Fig. 7 clearly shows some differences in gas phase and ice phase electronic absorption spectra of H_2Cl^+ .

4. CONCLUSIONS

Protonated hydrogen chloride or chloronium (H_2Cl^+) ion has been recently identified towards Sgr A, W31C. In this paper, we investigated the existence and different aspects of its two isotopomers namely, HDCl^+ and D_2Cl^+ . Following are the major results of this paper:

- Langevin theory and parameterized trajectory theory are used for the computation of various ion molecular reaction rates containing H_2Cl^+ and its related species.
- Our chemical modeling shows that HDCl^+ could be efficiently formed in gas phase and emission line should be strong enough to be observed.
- We explored vibrational, rotational and electronic spectral properties of H_2Cl^+ , D_2Cl^+ and HDCl^+ in different astrophysical environments. Resulting chemical parameters could assist observers in identifying these molecules around Interstellar Molecular cloud. In Appendix A, we present a representative catalog files in JPL format for gas phase HDCl^+ which will be useful for observational purpose.

5. ACKNOWLEDGMENTS

Ankan Das is grateful to ISRO for financial support through a respond project (Grant No. ISRO/RES/2/372/11-12), SKC thank a DST project (Grant No.SR/S2/HEP-40/2008) and LM thank MOES for partial funding during this work. The authors would like to thank the anonymous referee whose valuable suggestions have helped to improve this paper significantly.

REFERENCES

- Allamandola, L. J., Sandford S. A., Tielens A.G.G.M. 1992., APJ, 399, 134
 Albertsson, T., Semenov, D. A., Vasyunin, A. I., Henning T., Herbst, E., 2013, APJS, 207, 27
 Allen, M., Robinson, G. W., 1977., ApJ, 212, 396
 Amin, M. Y. 1996, Earth Moon Planets, 73, 133
 Asplund, M., Grevesse, N., Sauval, A. J., & Scott, P. 2009, ARA & A, 47, 481
 Blake, G. A., Keene, J., & Phillips, T. G. 1985, ApJ, 295, 501
 Blake, G. A., Anicich, V. G., & Huntress, W. T., Jr. 1986, ApJ, 300, 415
 Caselli, P., Stantcheva, T., Shalabiea, O., Shematovich, V. I. & Herbst, E., 2002, P&SS, 50, 1257
 Cazaux, S., Cobut, V., Marseille, M., Spaans, M., Caselli, P. 2010, A&A, 522, 74
 Chakrabarti, S., Chakrabarti, S.K., 2000a. A&A 354, L6
 Chakrabarti, S. K., Chakrabarti, S., 2000b. Ind. J. Phys 74B, 97
 Chakrabarti, S.K., Das, A., Acharyya, K., Chakrabarti, S., 2006, A&A, 457, 167
 Chakrabarti, S.K., Das, A., Acharyya, K., Chakrabarti, S., 2006, BASI, 34, 299
 Cuppen, H. M., Herbst, E., 2007, APJ, 668, 294
 Cuppen, H. M., Van Dishoeck E., F., Herbst, E., Tielens, A. G. G. M., 2009, A&A, 508, 275
 Das, A., Chakrabarti, S. K., Acharyya K. & Chakrabarti, S., 2008a, NEWA, 13, 457
 Das, A., Acharyya, K., Chakrabarti, S. & Chakrabarti, S. K., 2008b, A&A, 486, 209
 Das, A., Acharyya, K. & Chakrabarti, S. K., 2010, MNRAS 409, 789
 Das, A. & Chakrabarti, S. K., 2011, 418. 545, MNRAS
 Das, A., Majumdar, L., Chakrabarti, S. K., & Chakrabarti S., 2013a, NEWA, 23, 118
 Das, A., Majumdar, L., Chakrabarti, S. K., & Saha, R., Chakrabarti, S., 2013b, MNRAS, 433, 3152
 Dalgarno, A., de Jong, T., Oppenheimer, M., & Black, J. H. 1974, ApJ, 192, L37
 Draine, B. T. 1978, ApJS, 36, 595

TABLE 4

VIBRATIONAL FREQUENCIES OF DIFFERENT FORMS OF CHLORONIUM IN GAS PHASE, IN WATER ICE AND IN MIXED ICE AT MP2/AUG-CC-PVQZ LEVEL OF THEORY

Species	Charge	Spin state	Peak positions (Gas phase) (Wavenumber) (in cm^{-1})	Absorbance	Peak positions (H ₂ O ice) (Wavenumber) (in cm^{-1})	Absorbance	Peak positions (Mixed ice) (Wavenumber) (in cm^{-1})	Absorbance
H ₂ Cl ⁺	Cation	Singlet	1213.01	23.5567	1208.84	25.3066	1209.44	24.9379
			2779.83	342.2380	2822.06	409.2761	2818.33	403.9254
			2789.60	213.5581	2834.00	267.9801	2831.03	262.6758
D ₂ Cl ⁺	Cation	Singlet	870.12	8.0653	866.89	8.8043	867.34	8.6495
			1995.63	164.4252	2025.45	198.2665	2022.82	195.5651
			1998.19	100.4653	2030.55	127.2815	2028.39	124.6488
HDCl ⁺	Cation	Singlet	1055.58	21.0134	1051.30	23.6298	1051.20	23.2953
			1996.92	132.2521	2027.98	163.0641	2025.58	160.4419
			2784.69	278.3963	2828.05	338.3961	2824.70	333.0264

TABLE 5

THEORETICAL & AVAILABLE EXPERIMENTAL ROTATIONAL PARAMETERS OF CHLORONIUM AND ITS DIFFERENT ISOTOPOMERS AT MP2/AUG-CC-PVQZ LEVEL OF THEORY

Species	Rotational constants	Values in MHz	Experimental values in MHz ^a	Distortional constants	Values in MHz	Experimental values in MHz ^a
H ₂ Cl ⁺ in gas phase	A	336730.77093	337353.229	D_J	0.19899×10^2	-
	B	274941.86042	273586.425	D_{JK}	-0.73569×10^2	-71.814
	C	151335.22094	148100.004	D_K	0.12577×10^3	-
				d_1	-0.83773×10^1	-
				d_2	0.58014	-
HDCl ⁺ in gas phase	A	309898.96477		D_J	0.35636×10^1	
	B	153561.70202		D_{JK}	-0.92932×10^1	
	C	102697.60073		D_K	0.98535×10^2	
				d_1	-0.13938×10^1	
				d_2	-0.11650	
D ₂ Cl ⁺ in gas phase	A	177672.18281		D_J	0.48691×10^1	
	B	137566.23157		D_{JK}	-0.17934×10^2	
	C	77526.70474		D_K	0.33137×10^2	
				d_1	-0.20906×10^1	
				d_2	-0.81717×10^{-1}	

^a Saito & Yamamoto et al., (1988)

- de Graauw, Th., Helmich F. P., Phillips, T. G., et al. 2010, A & A, 518, L6
- Emprechtinger, M., Caselli, P., Volgenau, N. H., Stutzki, J., Wiedner, M. C., 2008, A&A, 493,89
- Froebrich, D. 2005, ApJS, 156, 169
- Federman, S. R., Cardell, J. A., van Dishoeck, E. F., Lambert, D. L., & Black, , ApJ, 1995 445, 325
- Foresman, J.B., Frisch, A., 1995-96, Exploring Chemistry with Electronic structure Gaussian, Inc., Pittsburgh, PA, 15106 USA
- Glenewinkel-Meyer T., Ottinger, C., Rosmus, P., Werner, H-J, 1991, Chem. Phys. 152 409
- Herbst, E. 2006, in Springer Handbook of Atomic, Molecular, and Optical Physics, ed. G. W. F. Drake (New York: Springer), 561
- Hasegawa, T.,Herbst, E., Leung, C.M., 1992, APJ, 82, 167
- Jura, M. 1974, ApJ, 190, L33
- Keane, J. V., Boogert, A. C. A., Tielens, A. G. G. M., Ehrenfreund, P., Schutte, W. A., 2001, A&A, 375L, 43
- Leitch-Devlin, M., A., Williams, D., A., 213, 295, MNRAS, 1985
- Lis, D. C., Pearson, J. C., Neufeld, D. A., et al. 2010, A & A, 521, L9
- Linsky, J.L., Diplas, A., Wood, B.E., Brown, A., Ayres, T.R., Savage, B.D., 1995. ApJ. 451, 335B351
- Majumdar, L., Das, A., Chakrabarti, S.K., Chakrabarti, S., 2013a, New Astronomy, 20, 15
- Majumdar, L., Das, A., Chakrabarti, S.K., 2013b, A&A (in press)
- Majumdar, L., Das, A., Chakrabarti, S.K., Chakrabarti, S., 2012, Research in Astronomy & Astrophysics, 12, 1613
- Müller, H. S. P., unpublished result reported on The Cologne Database
- Müller, H. S. P., Schloder, F., Stutzki, J., & Winnewisser, G. 2005, J. Mol. Struct., 742, 215
- Myers, P. C., Adams, F. C., Chen, H., et al. 1998, ApJ, 492, 703
- Muller, H. S. P., Thorwirth, S., Roth, D. A., & Winnewisser, G. 2001, A&A, 370, L49
- Neufeld, D. A., Goicoechea, J. R., Sonnentrucker, P., et al. 2010, A & A, 521, L10
- Neufeld, D. A., Wolfire, M. G. 2009, ApJ, 706, 1594
- Neufeld, D. A., Roueff, E., Shell, R. L. et al., 2012, ApJ, 748, 37
- Pascual-Ahuir, J. L., Silla, E., Tun, I., J. Comp. Chem., 1994, 15, 1127
- Pickett, H. M., J. Mol. Spectrosc., 1991, 148, 371
- Pilbratt, G. L., Riedinger, J. R., Passvogel, T., et al. 2010, A & A, 518, L1
- Puzzarini, C., Stanton, J. F., Gauss, J., 2010, International Review in Physical Chemistry, 29,2,273
- Roberts, H., Millar, T. J., 2000, A&A, 361, 388
- Salez, M., Frerking, M. A., & Langer, W. D. 1996, ApJ, 467, 708
- Saito, S., Yamamoto, S., 1988, J. Chem. Phys., 88, 2281
- Schilke, P., Phillips, T. G., & Wang, N. 1995, ApJ, 441, 334
- Shalabiea, O. M., Greenberg, J. M., 1994, A&A, 290, 266
- Smith, M. 1998, Ap&SS, 261, 169
- Sonnentrucker, P., Neufeld, D. A., Phillips, T. G., et al. 2010, A&A, 521, L12
- Stantcheva, T., Shematovich, V. I., Herbst, E., 2002, A&A, 391, 1069
- Su, T., & Chesnavich, W. J. 1982, J. Chem. Phys., 76, 5183
- Tomasi, J., Cammi, R., Mennucci, B., Cappelli, C., and Corni, S., Phys. Chem. Chem. Phys., 2002, 4, 5697

TABLE 6
ELECTRONIC TRANSITIONS OF H_2Cl^+ AT B3LYP/6-311++G** LEVEL OF THEORY

Species	Wavelength in nm	Absorbance	Oscillator strength	Transitions	Contribution in %
H_2Cl^+ in gas phase	113.9	4864.07	0.1201	H-1 \rightarrow L+0	98
	99.7	5322.96	0.1316	H-1 \rightarrow L+1	90
	90.6	11062.41	0.2728	H-0 \rightarrow L+2	100
	80.3	22614.49	0.5051	H-2 \rightarrow L+0	66
	76.1	27125.91	0.4172	H-1 \rightarrow L+3	70
	70.8	9307.55	0.211	H-2 \rightarrow L+1	57
	62.3	13154.01	0.2709	H-2 \rightarrow L+2	90
	57.3	1301.54	0.03	H-0 \rightarrow L+9	100
	53.3	4644.87	0.1117	H-1 \rightarrow L+8	96
	44.2	4413.36	0.1047	H-2 \rightarrow L+9	90
	36.4	9444.575	0.2395	H-0 \rightarrow L+13	100
	34.5	2347.95	0.0594	H-1 \rightarrow L+13	98
	32.09	1508.80	0.0205	H-3 \rightarrow L+10	100
	30.79	1549.00	0.0402	H-3 \rightarrow L+10	100
H_2Cl^+ in ice phase	113.3	5297.52	0.1308	H-1 \rightarrow L+0	98
	98.1	11706.04	0.513	H-0 \rightarrow L+2	97
	80.3	31995.46	0.7694	H-2 \rightarrow L+0	66
	72.6	18217.29	0.4457	H-2 \rightarrow L+1	83
	65.1	13505.80	0	H-2 \rightarrow L+4	74
	58.4	1618.54	0.0381	H-0 \rightarrow L+9	100
	55.0	4755.99	0.1215	H-1 \rightarrow L+8	96
	46.8	2349.30	0.0526	H-2 \rightarrow L+8	91
	45.2	4262.98	0	H-2 \rightarrow L+11	100
	40.21	697.86	0.018	H-2 \rightarrow L+12	48
	36.7	9872.20	0.2521	H-0 \rightarrow L+13	100
	34.7	2272.75	0.065	H-1 \rightarrow L+13	99
	32.9	1495.5532	0.0207	H-3 \rightarrow L+11	100
	31.4	1707.95	0.0437	H-3 \rightarrow L+12	82
H_2Cl^+ in mixed ice	113.5	5344.97	0.1321	H-1 \rightarrow L+0	98
	99.4	206.40	0.1575	H-1 \rightarrow L+1	92
	80.3	31849.63	0.7566	H-2 \rightarrow L+0	63
	72.6	18544.85	0.4527	H-2 \rightarrow L+1	82
	65.7	13565.30	0	H-2 \rightarrow L+5	100
	58.4	1616.83	0.0388	H-0 \rightarrow L+9	100
	54.9	4785.04	0.1193	H-1 \rightarrow L+8	96
	36.7	9833.04	0.2511	H-0 \rightarrow L+13	100

Tomasi, J., Mennucci, B., Cammi, R., Chem. Rev., 2005, 105, 2999
Tomasi, J., Mennucci, B., Cancs, E., J. Mol. Struct. (Theochem), 1999, 464, 211
van Dishoeck, E. F., & Black, J. H. 1986, ApJS, 62, 109

Woon, D. E., Herbst, E., 2009, APJS, 185, 273
Woodall, J., Agnede, M., Markwick-Kemper, A.J., Millar, T.J., 2007, A&A, 466, 1197
Zmuidzinas, J., Blake, G. A., Carlstrom, J., et al. 1995, ApJ, 447, L125

Appendix-A

Existence of interstellar Chloronium ion has recently been reported by Herschel Space Observatory's Heterodyne Instrument for Far-Infrared (Neufeld et al. 2012). Our calculations show that one of the deuterated forms of chloronium ion (HDCl^+) is significantly abundant and should be observed. In order to summarize results of our computation on rotational spectroscopy, we prepare our spectral information for HDCl^+ (Table A1 in the format of JPL catalog) to assist its detection around the ISM. In Table A1, the computed rotational transitions for the gas phase HDCl^+ is shown. This Table is prepared with our calculated values of spectroscopic constants which are given in Table 5. In Table A1, we have given the rotational transitions in MHz unit. Corresponding intensity of lines are tabulated in $\text{nm}^2 \text{ MHz}$ unit. Intensity of any line represents absorption cross section over spectral line shape (calculated at 300K and tabulated in base 10 logarithm unit). Other parameters which are responsible for the computation of line frequencies are given at footnote of Table A1.

Table A1: Different rotational transitions and its related parameters for gas phase HDCl^+ in the format of JPL catalog.

Frequency ^a	Uncertainty ^b	I ^c	D ^d	E _{lower} ^e	g _{up} ^f	Tag ^g	QnF ^h	Qn _{up} ⁱ	Qn _{lower} ^j
257376.1993	0.0000	-2.8248	3	-0.0000	4	38001	335	1 0 1 2 2	0 0 0 2 1
257376.1993	0.0000	-2.4316	3	-0.0000	4	38001	335	1 0 1 2 2	0 0 0 2 2
257376.1993	0.0000	-2.8248	3	-0.0000	4	38001	335	1 0 1 2 2	0 0 0 2 1
257376.1993	0.0000	-2.7830	3	-0.0000	4	38001	335	1 0 1 2 2	0 0 0 2 3
257376.2326	0.0000	-2.7797	3	-0.0000	6	38001	335	1 0 1 2 3	0 0 0 2 2
257376.2326	0.0000	-2.0650	3	-0.0000	6	38001	335	1 0 1 2 3	0 0 0 2 3
257376.2592	0.0000	-2.7200	3	-0.0000	2	38001	335	1 0 1 2 1	0 0 0 2 1
257376.2592	0.0000	-2.8187	3	-0.0000	2	38001	335	1 0 1 2 1	0 0 0 2 2
257386.0031	0.0000	-2.2865	3	-0.0000	4	38001	335	1 0 1 3 2	0 0 0 2 1
257386.0031	0.0000	-2.7946	3	-0.0000	4	38001	335	1 0 1 3 2	0 0 0 2 2
257386.0031	0.0000	-4.1421	3	-0.0000	4	38001	335	1 0 1 3 2	0 0 0 2 3
257386.0181	0.0000	-1.8634	3	-0.0000	8	38001	335	1 0 1 3 4	0 0 0 2 3
257386.0529	0.0000	-2.0650	3	-0.0000	6	38001	335	1 0 1 3 3	0 0 0 2 2
257386.0529	0.0000	-2.7796	3	-0.0000	6	38001	335	1 0 1 3 3	0 0 0 2 3
257393.8667	0.0000	-2.8187	3	-0.0000	2	38001	335	1 0 1 1 1	0 0 0 2 1
257393.8667	0.0000	-2.7199	3	-0.0000	2	38001	335	1 0 1 1 1	0 0 0 2 2
257393.8669	0.0000	-3.7450	3	-0.0000	4	38001	335	1 0 1 1 2	0 0 0 2 1
257393.8669	0.0000	-2.2901	3	-0.0000	4	38001	335	1 0 1 1 2	0 0 0 2 3
257393.8670	0.0000	-2.8123	3	-0.0000	4	38001	335	1 0 1 1 2	0 0 0 2 2
514659.8572	0.0000	-6.7938	3	8.5857	4	38001	335	2 0 2 3 2	1 0 1 1 1
514659.8824	0.0000	-7.4094	3	8.5857	6	38001	335	2 0 2 3 3	1 0 1 1 2
514666.8692	0.0000	-3.1365	3	8.5857	2	38001	335	2 0 2 2 1	1 0 1 1 2
514666.8694	0.0000	-1.7143	3	8.5857	6	38001	335	2 0 2 2 3	1 0 1 1 2
514666.8695	0.0000	-2.2435	3	8.5857	2	38001	335	2 0 2 2 1	1 0 1 1 1
514666.8696	0.0000	-2.2437	3	8.5857	4	38001	335	2 0 2 2 2	1 0 1 1 2
514666.8698	0.0000	-2.1448	3	8.5857	4	38001	335	2 0 2 2 2	1 0 1 1 1
514667.6710	0.0000	-2.8243	3	8.5855	4	38001	335	2 0 2 3 2	1 0 1 3 3
514667.6788	0.0000	-2.8208	3	8.5855	8	38001	335	2 0 2 3 4	1 0 1 3 3
514667.6964	0.0000	-1.9589	3	8.5855	6	38001	335	2 0 2 3 3	1 0 1 3 3
514667.7136	0.0000	-1.7698	3	8.5855	8	38001	335	2 0 2 3 4	1 0 1 3 4
514667.7208	0.0000	-2.1126	3	8.5855	4	38001	335	2 0 2 3 2	1 0 1 3 2
514667.7313	0.0000	-2.8220	3	8.5855	6	38001	335	2 0 2 3 3	1 0 1 3 4
514667.7463	0.0000	-2.8260	3	8.5855	6	38001	335	2 0 2 3 3	1 0 1 3 2
514669.6441	0.0000	-5.4590	3	8.5857	6	38001	335	2 0 2 4 3	1 0 1 1 2
514674.6834	0.0000	-3.6631	3	8.5855	6	38001	335	2 0 2 2 3	1 0 1 3 3
514674.6836	0.0000	-2.8877	3	8.5855	4	38001	335	2 0 2 2 2	1 0 1 3 3
514674.7183	0.0000	-2.6833	3	8.5855	6	38001	335	2 0 2 2 3	1 0 1 3 4
514674.7331	0.0000	-3.1158	3	8.5855	2	38001	335	2 0 2 2 1	1 0 1 3 2
514674.7332	0.0000	-4.5605	3	8.5855	6	38001	335	2 0 2 2 3	1 0 1 3 2
514674.7334	0.0000	-3.5845	3	8.5855	4	38001	335	2 0 2 2 2	1 0 1 3 2
514676.6697	0.0000	-1.8438	3	8.5857	4	38001	335	2 0 2 1 2	1 0 1 1 2
514676.6698	0.0000	-1.9425	3	8.5857	2	38001	335	2 0 2 1 1	1 0 1 1 2
514676.6699	0.0000	-1.9425	3	8.5857	4	38001	335	2 0 2 1 2	1 0 1 1 1
514676.6700	0.0000	-2.8364	3	8.5857	2	38001	335	2 0 2 1 1	1 0 1 1 1
514677.4582	0.0000	-2.3000	3	8.5855	6	38001	335	2 0 2 4 3	1 0 1 3 3
514677.4648	0.0000	-1.7918	3	8.5851	4	38001	335	2 0 2 3 2	1 0 1 2 1
514677.4913	0.0000	-3.6483	3	8.5851	4	38001	335	2 0 2 3 2	1 0 1 2 3
514677.4930	0.0000	-4.0096	3	8.5855	6	38001	335	2 0 2 4 3	1 0 1 3 4
514677.4991	0.0000	-1.3636	3	8.5851	8	38001	335	2 0 2 3 4	1 0 1 2 3
514677.5064	0.0000	-1.1122	3	8.5855	10	38001	335	2 0 2 4 5	1 0 1 3 4
514677.5080	0.0000	-1.3848	3	8.5855	6	38001	335	2 0 2 4 3	1 0 1 3 2
514677.5167	0.0000	-2.2922	3	8.5851	6	38001	335	2 0 2 3 3	1 0 1 2 3
514677.5172	0.0000	-1.2463	3	8.5855	8	38001	335	2 0 2 4 4	1 0 1 3 3
514677.5246	0.0000	-2.2754	3	8.5851	4	38001	335	2 0 2 3 2	1 0 1 2 2
514677.5500	0.0000	-1.5647	3	8.5851	6	38001	335	2 0 2 3 3	1 0 1 2 2
514677.5521	0.0000	-2.2942	3	8.5855	8	38001	335	2 0 2 4 4	1 0 1 3 4
514684.4770	0.0000	-2.3423	3	8.5851	2	38001	335	2 0 2 2 1	1 0 1 2 1
514684.4773	0.0000	-2.4262	3	8.5851	4	38001	335	2 0 2 2 2	1 0 1 2 1
514684.4837	0.0000	-7.6805	3	8.5855	4	38001	335	2 0 2 1 2	1 0 1 3 3
514684.5037	0.0000	-1.6815	3	8.5851	6	38001	335	2 0 2 2 3	1 0 1 2 3
514684.5039	0.0000	-2.4062	3	8.5851	4	38001	335	2 0 2 2 2	1 0 1 2 3
514684.5335	0.0000	-6.3471	3	8.5855	4	38001	335	2 0 2 1 2	1 0 1 3 2
514684.5337	0.0000	-7.0346	3	8.5855	2	38001	335	2 0 2 1 1	1 0 1 3 2
514684.5368	0.0000	-2.4322	3	8.5851	2	38001	335	2 0 2 2 1	1 0 1 2 2
514684.5370	0.0000	-2.4096	3	8.5851	6	38001	335	2 0 2 2 3	1 0 1 2 2
514684.5372	0.0000	-2.0557	3	8.5851	4	38001	335	2 0 2 2 2	1 0 1 2 2
514687.2785	0.0000	-5.8721	3	8.5851	6	38001	335	2 0 2 4 3	1 0 1 2 3
514687.3117	0.0000	-6.2690	3	8.5851	6	38001	335	2 0 2 4 3	1 0 1 2 2
514687.3375	0.0000	-7.5999	3	8.5851	8	38001	335	2 0 2 4 4	1 0 1 2 3
514694.2775	0.0000	-3.8539	3	8.5851	4	38001	335	2 0 2 1 2	1 0 1 2 1
514694.2776	0.0000	-2.9352	3	8.5851	2	38001	335	2 0 2 1 1	1 0 1 2 1
514694.3040	0.0000	-2.4123	3	8.5851	4	38001	335	2 0 2 1 2	1 0 1 2 3
514694.3373	0.0000	-2.9434	3	8.5851	4	38001	335	2 0 2 1 2	1 0 1 2 2
514694.3374	0.0000	-2.8496	3	8.5851	2	38001	335	2 0 2 1 1	1 0 1 2 2

Frequency ^a	Uncertainty ^b	I ^c	D ^d	E _{lower} ^e	g _{up} ^f	Tag ^g	QnF ^h	Qn _{up} ⁱ	Qn _{lower} ^j
771769.9945	0.0000	-7.6046	3	25.7535	6	38001	335	3 0 3 4 3	2 0 2 1 2
771774.5695	0.0000	-6.9643	3	25.7535	4	38001	335	3 0 3 3 2	2 0 2 1 1
771774.5696	0.0000	-6.7153	3	25.7535	4	38001	335	3 0 3 3 2	2 0 2 1 2
771776.9609	0.0000	-2.9249	3	25.7533	6	38001	335	3 0 3 4 3	2 0 2 4 4
771776.9716	0.0000	-2.9289	3	25.7533	10	38001	335	3 0 3 4 5	2 0 2 4 4
771777.0070	0.0000	-1.7710	3	25.7533	8	38001	335	3 0 3 4 4	2 0 2 4 4
771777.0173	0.0000	-1.6427	3	25.7533	10	38001	335	3 0 3 4 5	2 0 2 4 5
771777.0200	0.0000	-1.8814	3	25.7533	6	38001	335	3 0 3 4 3	2 0 2 4 3
771777.0527	0.0000	-2.9291	3	25.7533	8	38001	335	3 0 3 4 4	2 0 2 4 5
771777.0661	0.0000	-2.9252	3	25.7533	8	38001	335	3 0 3 4 4	2 0 2 4 3
771779.7946	0.0000	-8.0545	3	25.7532	6	38001	335	3 0 3 4 3	2 0 2 2 2
771779.7948	0.0000	-5.5854	3	25.7532	6	38001	335	3 0 3 4 3	2 0 2 2 3
771779.8409	0.0000	-6.5020	3	25.7532	8	38001	335	3 0 3 4 4	2 0 2 2 3
771781.5480	0.0000	-4.2055	3	25.7533	8	38001	335	3 0 3 3 4	2 0 2 4 4
771781.5754	0.0000	-3.0578	3	25.7533	6	38001	335	3 0 3 3 3	2 0 2 4 4
771781.5937	0.0000	-2.9173	3	25.7533	8	38001	335	3 0 3 3 4	2 0 2 4 5
771781.5952	0.0000	-3.2034	3	25.7533	4	38001	335	3 0 3 3 2	2 0 2 4 3
771781.6070	0.0000	-7.8321	3	25.7533	8	38001	335	3 0 3 3 4	2 0 2 4 3
771781.6345	0.0000	-3.9561	3	25.7533	6	38001	335	3 0 3 3 3	2 0 2 4 3
771784.3550	0.0000	-1.6817	3	25.7535	2	38001	335	3 0 3 2 1	2 0 2 1 1
771784.3551	0.0000	-2.5820	3	25.7535	2	38001	335	3 0 3 2 1	2 0 2 1 2
771784.3698	0.0000	-1.9214	3	25.7532	4	38001	335	3 0 3 3 2	2 0 2 2 2
771784.3699	0.0000	-3.2816	3	25.7532	4	38001	335	3 0 3 3 2	2 0 2 2 3
771784.3701	0.0000	-1.4255	3	25.7532	4	38001	335	3 0 3 3 2	2 0 2 2 1
771784.3817	0.0000	-1.1519	3	25.7535	6	38001	335	3 0 3 2 3	2 0 2 1 2
771784.3818	0.0000	-0.9989	3	25.7532	8	38001	335	3 0 3 3 4	2 0 2 2 3
771784.4091	0.0000	-1.1980	3	25.7532	6	38001	335	3 0 3 3 3	2 0 2 2 2
771784.4092	0.0000	-1.9191	3	25.7532	6	38001	335	3 0 3 3 3	2 0 2 2 3
771784.4147	0.0000	-1.5815	3	25.7535	4	38001	335	3 0 3 2 2	2 0 2 1 1
771784.4149	0.0000	-1.6789	3	25.7535	4	38001	335	3 0 3 2 2	2 0 2 1 2
771786.7559	0.0000	-2.0839	3	25.7533	8	38001	335	3 0 3 5 4	2 0 2 4 4
771786.7817	0.0000	-2.0168	3	25.7529	6	38001	335	3 0 3 4 3	2 0 2 3 3
771786.7994	0.0000	-3.6919	3	25.7529	6	38001	335	3 0 3 4 3	2 0 2 3 4
771786.8016	0.0000	-3.9953	3	25.7533	8	38001	335	3 0 3 5 4	2 0 2 4 5
771786.8072	0.0000	-1.1157	3	25.7529	6	38001	335	3 0 3 4 3	2 0 2 3 2
771786.8101	0.0000	-0.8416	3	25.7529	10	38001	335	3 0 3 4 5	2 0 2 3 4
771786.8131	0.0000	-0.6956	3	25.7533	12	38001	335	3 0 3 5 6	2 0 2 4 5
771786.8150	0.0000	-0.8996	3	25.7533	8	38001	335	3 0 3 5 4	2 0 2 4 3
771786.8180	0.0000	-0.7969	3	25.7533	10	38001	335	3 0 3 5 5	2 0 2 4 4
771786.8278	0.0000	-0.9754	3	25.7529	8	38001	335	3 0 3 4 4	2 0 2 3 3
771786.8455	0.0000	-2.0349	3	25.7529	8	38001	335	3 0 3 4 4	2 0 2 3 4
771786.8637	0.0000	-2.0790	3	25.7533	10	38001	335	3 0 3 5 5	2 0 2 4 5

^a Calculated frequency in MHz

^b Calculated uncertainty of the line. If the line position is in units of MHz then uncertainty of the line is greater or equal to zero.

^c Base 10 logarithm of the integrated intensity at 300K in nm² MHz

^d Degrees of freedom in the rotational partition function (0 for atoms, 2 for linear molecules, 3 for non linear molecules)

^e Lower state energy in cm⁻¹ relative to the lowest energy level in the ground vibronic state.

^f Upper state degeneracy : $g_{up} = g_I \times g_N$, where g_I is the spin statistical weight and $g_N = 2N + 1$ the rotational degeneracy.

^g Molecule Tag

^h Coding for the format of quantum numbers.

$QnF = 100 \times Q + 10 \times H + N_{Qn}$; N_{Qn} is the number of quantum numbers for each state; H indicates the number of half integer quantum numbers; $Q \bmod 5$, the residual when Q is divided by 5, gives the number of principal quantum numbers (without the spin designating ones)

ⁱ Quantum numbers for the upper state

^j Quantum numbers for the lower state